Published in final edited form as:
*Oncogene*. 2007 September 13; 26(42): 6238–6243. doi:10.1038/sj.onc.1210429.

# Prostate cancer specific integrin *αvβ3* modulates bone metastatic growth and tissue remodeling

**NP McCabe**[1], **S De**[1], **A Vasanji**[2], **J Brainard**[3], and **TV Byzova**[1]

[1]Department of Molecular Cardiology, Joseph J Jacobs Center for Thrombosis and Vascular Biology, Cleveland Clinic Foundation, Cleveland, OH, USA

[2]Department of Biomedical Engineering, Cleveland Clinic Foundation, Cleveland, OH, USA

[3]Department of Anatomic Pathology, Cleveland Clinic Foundation, Cleveland, OH, USA

## Abstract

The management of pain and morbidity owing to the spreading and growth of cancer within bone remains to be a paramount problem in clinical care. Cancer cells actively transform bone, however, the molecular requirements and mechanisms of this process remain unclear. This study shows that functional modulation of the *αvβ3* integrin receptor in prostate cancer cells is required for progression within bone and determines tumor-induced bone tissue transformation. Using histology and quantitative microCT analysis, we show that *αvβ3* integrin is required not only for tumor growth within the bone but for tumor-induced bone gain, a response resembling bone lesions in prostate cancer patients. Expression of normal, fully functional *αvβ3* enabled tumor growth in bone (incidence: 4/4), whereas *αvβ3* (—), inactive or constitutively active mutants of *αvβ3* did not (incidence: 0/4, 0/6 and 1/7, respectively) within a 35-day-period. This response appeared to be bone-specific in comparison to the subcutis where tumor incidence was greater than 60% for all groups. Interestingly, bone residing prostate cancer cells expressing normal or dis-regulated *αvβ3* (either inactive of constitutively active), but not those lacking *β3* promoted bone gain or afforded protection from bone loss in the presence or absence of histologically detectable tumor 35 days following implantation. As bone is replete with ligands for *β3* integrin, we next demonstrated that *αvβ3* integrin activation on tumor cells is essential for the recognition of key bone-specific matrix proteins. As a result, prostate cancer cells expressing fully functional but not dis-regulated *αvβ3* integrin are able to control their own adherence and migration to bone matrix, functions that facilitate tumor growth and control bone lesion development.

### Keywords

prostate cancer; metastasis; bone; integrins

The likelihood that patients with advanced prostate cancer will develop secondary lesions within the skeletal compartment is greater than 80% (Jacobs, 1983), thus indicating bone as a hospitable environment for the growth of disseminated disease. For successful engraftment within bone, prostate cancer cells must rely upon extracellular cues transmitted through growth factor receptors and cell adhesion molecules. Integrins are cell surface receptors that become



Correspondence: Dr TV Byzova, Department of Molecular Cardiology, Joseph J. Jacobs Center for Thrombosis and Vascular Biology, Cleveland Clinic Foundation, 9500 Euclid Avenue, Cleveland, OH 44195, USA. E mail: byzovat@ccf.org.

Supplementary Information accompanies the paper on the Oncogene website (http://www.nature.com/onc).

activated through a tightly regulated process involving intracellular signal induced conformational changes (Ginsberg *et al*., 1992), which results in the rapid modulation of integrin ligand-binding affinity. Ligand binding then initiates internalization of extracellular signals, which modulate multiple cellular processes associated with the metastatic phenotype such as adhesion, migration and invasion. Therefore, by regulating the adhesiveness of prostate cancer cells during various phases of the metastatic process, integrins can govern the process of dissemination. Prostate cancer colonization of bone initiates the deposition of new bone leading to morbidities such as bone pain, compression of the spinal cord, pathologic fracture and paralysis (Saad *et al*., 2006). New bone deposition occurs as existing bone is destroyed (Keller and Brown, 2004) through osteoclast-mediated resorption, which requires functional integrin $\alpha v\beta 3$ (Feng *et al*., 2001). In addition to its role in bone resorption, osteoclast $\alpha v\beta 3$ appears to play a role in tumor colonization and growth within bone (Bakewell *et al*., 2003).

Recent studies have shown that the expression of $\alpha v\beta 3$ promotes spontaneous metastasis of breast cancer to bone (Takayama *et al*., 2005; Sloan *et al*., 2006) and the functional state of integrin $\alpha v\beta 3$ is critical in many facets of this process. For example, constitutive activation of $\alpha v\beta 3$ on breast cancer cells (Felding-Habermann *et al*., 2001) promotes hematogenous dissemination of breast cancer by facilitating tumor cell arrest via interaction with platelets (Felding-Habermann *et al*., 2001). Previous studies have focused on expression and functional status of tumor-specific $\alpha v\beta 3$ in the hematogenous spread of cancers through observing bone homing potential. However, the role of tumor-specific $\alpha v\beta 3$ in processes such as cancer progression within bone and tumor induced bone remodeling has been overlooked.

This study was designed to establish the biological significance of the expression and functional state of prostate cancer-specific $\alpha v\beta 3$ on tumor growth and tumor-induced remodeling of bone. The preparation of cells used in this study have been described previously (De *et al*., 2005). In short, we have generated LNCaP C4–2 prostate cancer cells that have lost $\beta 3$ expression and used them to re-express (1) $\beta 3$ WT, which can form heterodimers with $\alpha v$ to form $\alpha v\beta 3$ in a relaxed, activatable state ($\alpha v\beta 3$ WT cells); (2) mutant $\beta 3$ D723R, which locks $\alpha v\beta 3$ in the activated state (Hughes *et al*., 1996) thus bypassing inside-out signaling ($\alpha v\beta 3$ constitutively active (CA) cells); or (3) mutant S752P, which locks $\alpha v\beta 3$ in the relaxed state (Chen *et al*., 1992) resulting in non-active integrin ($\alpha v\beta 3$ inactive cells). Flow cytometry indicated that expression levels of $\alpha v\beta 3$ in cells re-expressing $\beta 3$ integrin, whether WT, CA or inactive, were similar; however, fibrinogen binding was threefold higher for $\alpha v\beta 3$ CA cells compared to $\alpha v\beta 3$ WT cells (Supplementary Table 1). We have previously shown the activating nature of the $\beta 3$ D723R mutation by illustrating clustering characteristics of $\alpha v\beta 3$ CA in unstimulated C4–2 cells in suspension (De *et al*., 2005). We further confirmed the nature of this mutation by demonstrating constitutive phosphorylation of focal adhesion kinase following ligand binding (Supplementary Figure 1), an effect previously noted to be the result of constitutive integrin activation (Li *et al*., 2005). Thus, functional differences in $\alpha v\beta 3$ between WT, CA and inactive cells are critical in this model, not expression changes among these groups.

Microcomputed tomography (microCT) was used to monitor tumor-induced changes in bone structural indices over time. To obtain baseline bone structural indices, microCT analysis was performed 1-day post-intratibial implantation of prostate cancer cells. Contralateral tibiae were injected with vehicle to account for surgically induced remodeling. We found a wide range among multiple bone structural indices across the sample population of mice ($n$=19) upon initial scanning of the volume of interest. For example, the trabecular thickness in $\mu$m (range=45.25–76.69, mean=60.17±7.05 (s.d.)), trabecular spacing in $\mu$m (range=46.95–130.96, mean=86.85±20.55 (s.d.)), trabecular number per mm (range=9.64–16.97, mean=12.45±1.90 (s.d.)), and trabecular bone surface area in $mm^2$ (range=3.04–8.59, mean=6.02±1.34 (s.d.)) within individual tibiae varied drastically; however, no significant difference between the tibiae (right vs left) of individual animals was found. To account for

these inherent differences in bone structural indices, we expressed our data as percent differences in vehicle and tumor injected tibiae over time. Representative three-dimensional microCT images of tumor injected tibia from each group are shown in Figure 1 and changes in bone structural indices are in Table 1. As shown in Figure 2a, intratibial injection of $\alpha v\beta 3$ (—) tumor cells resulted in a bone fraction (% bone in the volume of interest) loss of ~14% whereas the three other groups ($\alpha v\beta 3$ WT, $\alpha v\beta 3$ inactive and $\alpha v\beta 3$ CA) displayed a moderate bone gain (15–28%). In addition, a 50% decrease in the number of trabeculae was observed in tibiae injected with $\alpha v\beta 3$ (—) cells, whereas a 35% increase in the number of trabeculae was observed in tibiae injected with $\alpha v\beta 3$ WT cells compared to mock-injected limbs (Figure 2b). Although prostate cancer cells expressing dis-regulated $\alpha v\beta 3$ demonstrated modest elevations in trabecular number accompanied with reductions in trabecular spacing (Table 1), bone gains were not significant. Significant differences in trabecular density were present when intergroup comparisons were made for change in spacing (C4–2 — PBS control) of C4–2 $\alpha v\beta 3$ (—) injected tibia vs that of $\alpha v\beta 3$ WT or inactive injected tibiae, but not when comparisons between C4–2 and control injected tibiae between animals within the same group were considered. This may be due to differences in tumor growth within injected tibiae as discussed below. Taken together, our data indicate that prostate cancer cells lacking $\alpha v\beta 3$ integrin expression promote bone loss, whereas the presence of tumor-specific $\alpha v\beta 3$ promotes bone deposition, thus illustrating a prominent role for tumor-specific $\alpha v\beta 3$ integrin in the development of osteoblastic bone lesions.

Tibiae were also examined histologically to determine tumor incidence (Figure 3). Cells lacking $\alpha v\beta 3$ expression as well as those expressing $\alpha v\beta 3$ CA or $\alpha v\beta 3$ inactive exhibited severely impaired tumor-forming potential in bone. Overall, these observations are consistent with the findings of others. Lack of $\alpha v\beta 3$ activity via expression as an inactive conformer results in severely impaired ligand binding and signal internalization (Chen *et al.*, 1992), and reduces tumor-forming potential in bone (Pecheur *et al*., 2002). Also, our observation of impaired tumor-forming potential of CA $\alpha v\beta 3$ expressing prostate cancer cells is in agreement with several other studies regarding the deleterious effects of CA $\beta 3$ integrins on long-term tumor cell survival (Kanamori *et al*., 2004) and integrin function *in vivo* (Ruiz *et al*., 2001). In contrast to cells expressing dis-regulated $\alpha v\beta 3$, C4–2 $\alpha v\beta 3$ WT cells (Figure 3a) displaced normal marrow cells of the tibial metaphysis to fill 75–90% of the bone cavity, penetrated the cortex and invaded adjacent soft tissue. Immunohistochemical detection of prostate-specific membrane antigen (PSMA) verified the presence of C4–2 $\alpha v\beta 3$ WT cells in the marrow space (Figure 3a). PSMA expression levels of the C4–2 lines used in our experiments were all similar as determined by immunoblotting (not shown). Despite the undetectable presence of tumor in $\alpha v\beta 3$ inactive and CA cell-injected tibiae in the majority of animals, it is possible that a brief growth period affords protection from bone destruction as tibiae injected with dis-regulated $\alpha v\beta 3$ cells showed resistance to bone loss compared to tibiae injected with $\alpha v\beta 3$ (—) cells as illustrated in Table 1 and Figure 2. In sum, expression of fully functional $\alpha v\beta 3$ WT integrin but not its dis-regulated conformers enable tumor progression in bone. The presence of $\alpha v\beta 3$ WT on prostate cancer cells also promoted tumorigenicity and growth in the subcutis (incidence 12/12; mean=0.71±0.14 g (s.d.); $P<0.01$ compared to $\alpha v\beta 3$ (—) tumors), a distinctly different environment from bone, while loss of $\alpha v\beta 3$ (incidence: 3/5; mean=0.12±0.03 g (s.d.)), or expression of $\alpha v\beta 3$ CA (incidence: 8/12; mean=0.11±0.06 g (s.d.); $P=0.75$ compared to $\alpha v\beta 3$ (—) tumors) or $\alpha v\beta 3$ inactive (incidence: 8/12; mean=0.18±0.07g (s.d.); $P=0.20$ compared to $\alpha v\beta 3$ (—) tumors) reduced tumorigenicity. Representative tumors are shown in Figure 3b. Although our *in vitro* findings indicate that proliferation among the C4–2 variants used in our study are similar (not shown), we cannot conclude that the cell lines have similar growth rates *in vivo*. Thus, functional regulation of prostate cancer $\alpha v\beta 3$ appears to determine tumorigenicity and is especially important in tissues rich in $\alpha v\beta 3$ ligands such as bone.

The abundance of αvβ3 ligands in bone may explain the attraction of both prostate and breast carcinomas to this tissue. We found that the activation status of αvβ3 plays a role in the adhesion and migration to individual bone matrix proteins and total bone extracts. Cells expressing constitutively active αvβ3 promoted robust cellular adhesion to vitronectin, a reference ligand for αvβ3 and major extracellular component of mature bone (Supplementary Table 2), whereas αvβ3 WT cells required stimulation to achieve the same effect. In addition, migration to vitronectin was dependent upon the activation state of αvβ3. In accordance with a previous study (Byzova *et al*., 2000), migration to bone sialoprotein (BSP) occurred in a concentration-dependent manner for αvβ3 WT and CA cells, whereas migration of αvβ3 (—) and αvβ3-inactive cells was negligible (Supplementary Table 2). In the presence of blocking antibody to αvβ3 (LM609), all cell types displayed similar levels of migration, indicating that αvβ3 is the specific integrin responsible for the observed migration. Migration of tumor cells to secreted protein acidic and rich in cysteine (SPARC) mirrored that of cells to BSP with SPARC promoting migration of αvβ3 WT and CA cells but not αvβ3 (—) cells. Pretreatment of αvβ3 WT and CA cells with LM609 resulted in decreased migration by approximately 70% indicating specificity. Little effect was noted in αvβ3 (—) and αvβ3-inactive cells. To ensure that our results were not owing to the use of isolated bone-derived proteins and thus do not reflect the milieu of bone constituents that prostate cancer cells would encounter upon entrance to the skeletal compartment, we confirmed our adhesion and migration results using total bone extract. Results from adhesion and migration experiments utilizing total bone extract mirrored and support those where isolated bone-derived proteins were used.

It is possible that αvβ3-inactive cells, which fail to transmit survival signals as a result of inefficient ligand binding (Chen *et al*., 1992) and express low levels of growth factors such as VEGF as a result of reduced αvβ3 ligand affinity (De *et al*., 2005), leads to a diminished capacity for long-term survival in bone (Kitagawa *et al*., 2005). Conversely, αvβ3 WT cells, which readily colonize bone, efficiently bind and migrate to ligand following αvβ3 activation. Interestingly, our adhesion and migration data indicated that αvβ3 CA cells should thrive within bone; however, αvβ3 CA cells exhibited a severely diminished capacity for sustained *in vivo* bone colonization. Our previous studies indicated that bone metastatic prostate cancer, in comparison to normal matched prostate tissue, expressed dramatically elevated levels of activated αvβ3 (De *et al*., 2003). This activation, however, was due to a feedback mechanism wherein VEGF signaling initiates inside-out αvβ3 activation leading to enhanced ligand-binding affinity. A constitutively active mutant of αvβ3 would bypass the need for activation and could not dynamically regulate cell adhesion, a condition, which may be deleterious for long term *in vivo* persistence in bone (Schwartz and Ginsberg, 2002). It is possible that constitutively active αvβ3, in the context of abundant matrix bound ligands such as that in bone, may lead to excessive, unregulated outside-in signaling that could be detrimental to tumor growth. Thus, expression of inactive αvβ3 by prostate cancer cells may inhibit sustained bone colonization and proliferation in bone tissue, whereas expression of constitutively active αvβ3 by prostate cancer cells may promote metastasis and initial engraftment within bone but inhibit subsequent growth.

Together, our data suggest that, in addition to elevated expression/usage of αvβ3 by bone metastatic prostate cancer cells (Stewart *et al*., 2004), the ability to regulate the recognition of extracellular matrix through physiological αvβ3 activation, a function lacking in both αvβ3 CA and αvβ3-inactive tumor cells, increases the potential for the development of skeletal metastases and contributes to the osteoblastic phenotype of bone lesions. Furthermore, we provide evidence that the activation status of integrin αvβ3 on prostate cancer cells influences recognition of individual bone matrix proteins, a key early step in the establishment of bone metastatic disease. Hence, integrin αvβ3 supports the development of bone metastases by at least three different mechanisms: (1) tumor-specific αvβ3 expression and functional state control prostate cancer engraftment of bone, survival following colonization, and tumor induce

tissue remodeling (present study); (2) osteoclast $\alpha v\beta 3$ activity controls bone resorption (Feng *et al*., 2001), a necessary event for the expansion of bone residing tumor and (3) osteoclast $\alpha v\beta 3$ enables the metastatic colonization and growth of tumor in bone (Bakewell *et al*., 2003). Considering these data, it is possible that antagonism of $\alpha v\beta 3$, thus inhibiting bone colonization (by acting upon prostate cancer cells and osteoclasts) and limiting proliferation of bone residing prostate cancer cells (Nemeth *et al*., 2003), coupled with one or more existing therapies could prove to be an effective, multifaceted treatment modality for patients with advanced disease.

## Supplementary Material

Refer to Web version on PubMed Central for supplementary material.

## Acknowledgements

We thank Dr Sara Seidelmann for critical review of this manuscript. This work was supported by the following grants: DK060933 to TV Byzova. NP McCabe is the recipient of a Ruth L Kirschstein Research Service Award (NRSA) Individual Fellowship (CA1172462); Cleveland Clinic Musculoskeletal Core Center funded in part by NIAMS Core Center Grant 1P30 AR-050953.

## References

Bakewell SJ, Nestor P, Prasad S, Tomasson MH, Dowland N, Mehrotra M, et al. Platelet and osteoclast beta3 integrins are critical for bone metastasis. Proc Natl Acad Sci USA 2003;100:14205–14210. [PubMed: 14612570]

Byzova TV, Kim W, Midura RJ, Plow EF. Activation of integrin alpha(V)beta(3) regulates cell adhesion and migration to bone sialoprotein. Exp Cell Res 2000;254:299–308. [PubMed: 10640428]

Chen YP, Djaffar I, Pidard D, Steiner B, Cieutat AM, Caen JP, et al. Ser-752—>Pro mutation in the cytoplasmic domain of integrin beta 3 subunit and defective activation of platelet integrin alpha IIb beta 3 (glycoprotein IIb-IIIa) in a variant of Glanzmann thrombasthenia. Proc Natl Acad Sci USA 1992;89:10169–10173. [PubMed: 1438206]

De S, Chen J, Narizhneva NV, Heston W, Brainard J, Sage EH, et al. Molecular pathway for cancer metastasis to bone. J Biol Chem 2003;278:39044–39050. [PubMed: 12885781]

De S, Razorenova O, McCabe NP, O'Toole T, Qin J, Byzova TV. VEGF-integrin interplay controls tumor growth and vascularization. Proc Natl Acad Sci USA 2005;102:7589–7594. [PubMed: 15897451]

Felding-Habermann B, O'Toole TE, Smith JW, Fransvea E, Ruggeri ZM, Ginsberg MH, et al. Integrin activation controls metastasis in human breast cancer. Proc Natl Acad Sci USA 2001;98:1853–1858. [PubMed: 11172040]

Feng X, Novack DV, Faccio R, Ory DS, Aya K, Boyer MI, et al. A Glanzmann's mutation in beta 3 integrin specifically impairs osteoclast function. J Clin Invest 2001;107:1137–1144. [PubMed: 11342577]

Ginsberg MH, Du X, Plow EF. Inside-out integrin signalling. Curr Opin Cell Biol 1992;4:766–771. [PubMed: 1419055]

Hughes PE, Diaz-Gonzalez F, Leong L, Wu C, McDonald JA, Shattil SJ, et al. Breaking the integrin hinge. A defined structural constraint regulates integrin signaling. J Biol Chem 1996;271:6571–6574. [PubMed: 8636068]

Jacobs SC. Spread of prostatic cancer to bone. Urology 1983;21:337–344. [PubMed: 6340324]

Kanamori M, Vanden Berg SR, Bergers G, Berger MS, Pieper RO. Integrin beta3 overexpression suppresses tumor growth in a human model of gliomagenesis: implications for the role of beta3 overexpression in glioblastoma multiforme. Cancer Res 2004;64:2751–2758. [PubMed: 15087390]

Keller ET, Brown J. Prostate cancer bone metastases promote both osteolytic and osteoblastic activity. J Cell Biochem 2004;91:718–729. [PubMed: 14991763]

Kitagawa Y, Dai J, Zhang J, Keller JM, Nor J, Yao Z, et al. Vascular endothelial growth factor contributes to prostate cancer-mediated osteoblastic activity. Cancer Res 2005;65:10921–10929. [PubMed: 16322239]

Latson, LKB.; Bryan, J.; Stredney, D.; Davros, W.; Midura, R.; Apte, S., et al. Proceedings of the 25th International Conference of the IEEE Engineering in Medicine and Biology Society; 2003. p. 1058-1061.

Li W, Metcalf DG, Gorelik R, Li R, Mitra N, Nanda V, et al. A push-pull mechanism for regulating integrin function. Proc Natl Acad Sci USA 2005;102:1424–1429. [PubMed: 15671157]

Nemeth JA, Cher ML, Zhou Z, Mullins C, Bhagat S, Trikha M. Inhibition of alpha(v)beta3 integrin reduces angiogenesis, bone turnover, and tumor cell proliferation in experimental prostate cancer bone metastases. Clin Exp Metastasis 2003;20:413–420. [PubMed: 14524530]

Pecheur I, Peyruchaud O, Serre CM, Guglielmi J, Voland C, Bourre F, et al. Integrin alpha(v)beta3 expression confers on tumor cells a greater propensity to metastasize to bone. FASEB J 2002;16:1266–1268. [PubMed: 12153995]

Ruiz C, Liu CY, Sun QH, Sigaud-Fiks M, Fressinaud E, Muller JY, et al. A point mutation in the cysteine-rich domain of glycoprotein (GP) IIIa results in the expression of a GPIIb-IIIa (alphaIIbbeta3) integrin receptor locked in a high-affinity state and a Glanzmann thrombasthenia-like phenotype. Blood 2001;98:2432–2441. [PubMed: 11588040]

Saad F, Clarke N, Colombel M. Natural history and treatment of bone complications in prostate cancer. Eur Urol 2006;49:429–440. [PubMed: 16431012]

Schwartz MA, Ginsberg MH. Networks and crosstalk: integrin signalling spreads. Nat Cell Biol 2002;4:E65–E68. [PubMed: 11944032]

Sloan EK, Pouliot N, Stanley KM, Chia J, Moseley JM, Hards DK, et al. Tumor-specific expression of $\alpha v\beta 3$ integrin promotes spontaneous metastasis of breast cancer to bone. Breast Cancer Res 2006;8:R20. [PubMed: 16608535]

Stewart DA, Cooper CR, Sikes RA. Changes in extracellular matrix (ECM) and ECM-associated proteins in the metastatic progression of prostate cancer. Reprod Biol Endocrinol 2004;2:2. [PubMed: 14711377]

Takayama S, Ishii S, Ikeda T, Masamura S, Doi M, Kitajima M. The relationship between bone metastasis from human breast cancer and integrin alpha(v)beta3 expression. Anticancer Res 2005;25:79–83. [PubMed: 15816522]

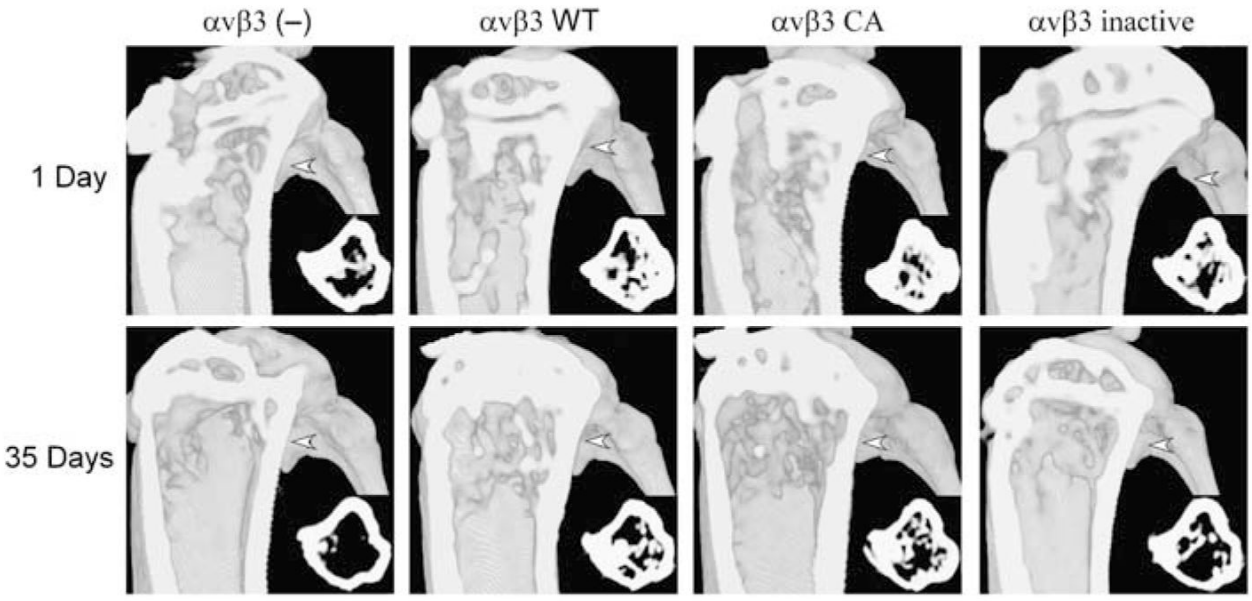


**Figure 1.**

*In vivo* bone imaging using microCT. Eight-week-old-male NOD CB17PRK Scid/J mice (Jackson Laboratories, Bar Harbor, ME, USA) were injected intratibially with C4–2 cells ($2.5 \times 10^5$ in 20 $\mu$l PBS). Contralateral tibiae were injected with PBS alone. Mice were anesthetized and secured on the rotating platform of a custom-designed microCT system (Latson *et al*., 2003). Three-dimensional reconstructions of 2D image stacks of injected tibiae 1 day and 35 days post-implantation of C4–2 cells are shown. The foreground is clipped to give a sagittal view of the bone cavity from the medial side. Insets depict transverse slices (medial is down, anterior is left) corresponding to the plane designated by white arrows.

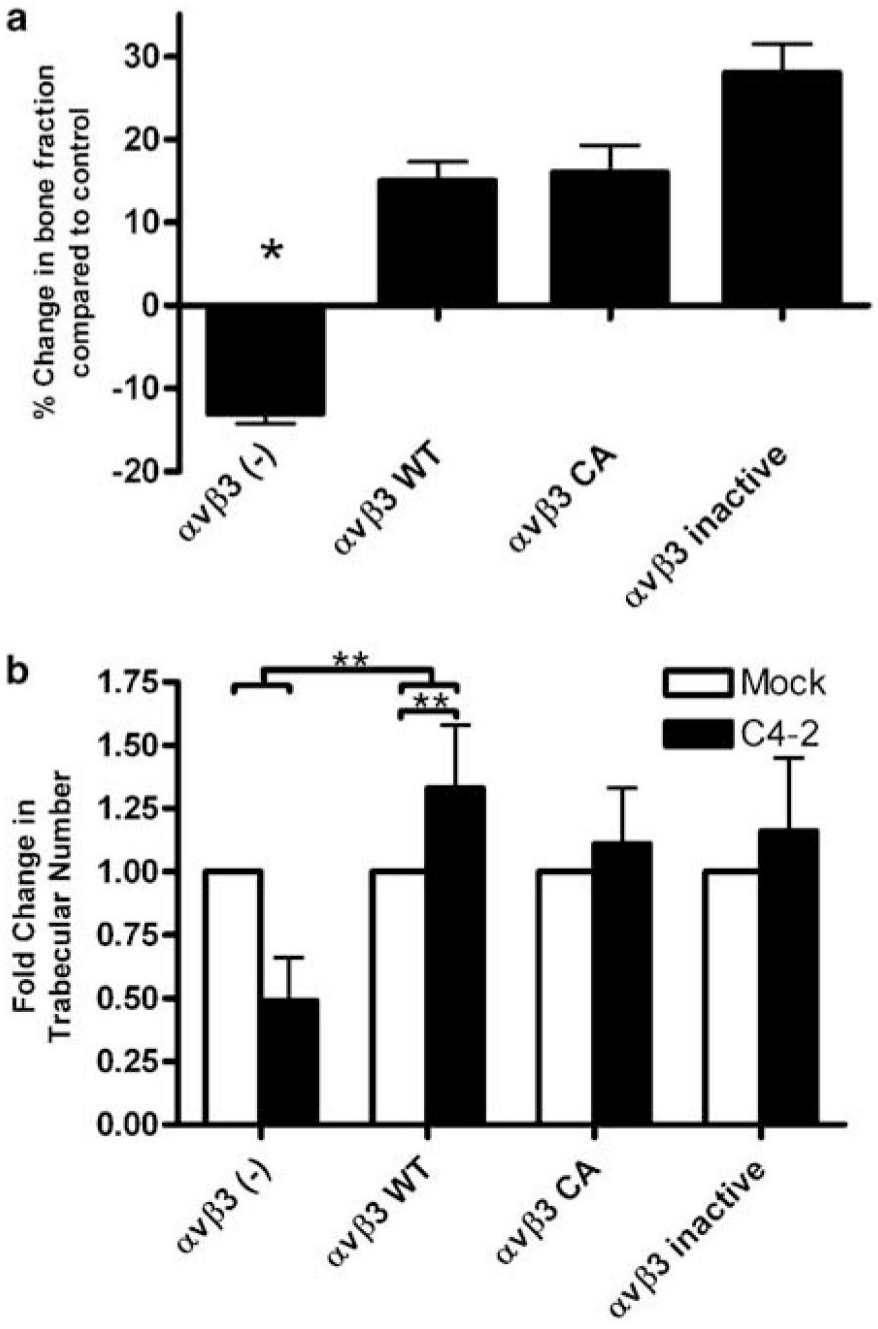


**Figure 2.**

MicroCT analysis of changes in bone structural indices. Tibial segmentation from surrounding bone, volume enhancement and delineation of volumes-of-interest (VOIs) were performed using open-source 3D visualization software (VolSuite, Ohio Supercomputer Center, Columbus, OH, USA). For each sample, a plane perpendicular to the *z* axis/tibial shaft was generated and placed at the base of the growth plate. A second, parallel plane was defined ~1.0 mm below the first and the entire volume was clipped to this VOI for quantitative analysis. (**a**) Changes in bone fraction of tibiae over a 35-day-period following injection with C4–2 prostate cancer cells lacking or expressing *αvβ3* integrin in different functional states. **P*<0.05

vs PBS control injections within the same group. (**b**) Changes in the number of trabeculae in the same bones as in (**a**). ***P*<0.01 vs PBS control injections within the same group or change in trabecular number of control vs C4–2 injected within the C4–2 $\alpha v\beta 3$ WT group compared to the same change within the $\alpha v\beta 3$ (—) group.

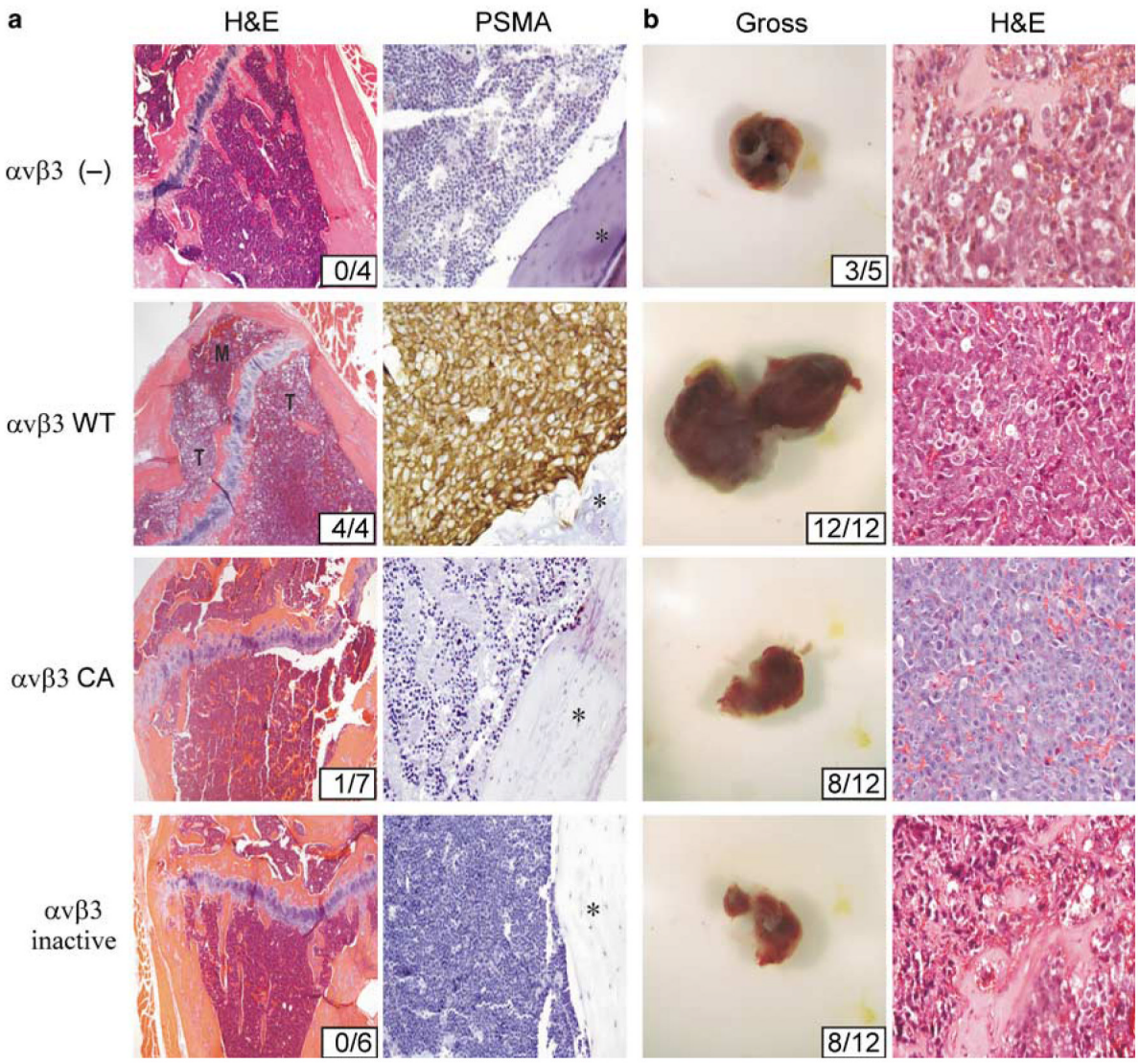


**Figure 3.**

Impairment of tumor growth as a consequence of *αvβ3* function is specific to the bone microenvironment. Intratibial injections were as described in Figure 1. Alternatively, mice were injected subcutaneously (sc) with matrigel suspensions of $1\times10^6$ C4–2 cells. (**a**) Left column: representative H&E histology of injected tibiae. Note that the majority of normal marrow (M) has been displaced by tumor (T) in the C4–2 *αvβ3* WT injected tibia (second row). Tumor incidence is shown in insets. Original magnification of ×20. Right column: tumor presence was confirmed immunohistochemically for the presence of PSMA. Asterisks indicate cortical bone. Original magnification of ×40. (**b**) Left column. Gross tumor analysis 4 weeks following injection of C4–2 cells. Tumor incidence is indicated in the inset. Right column: hematoylxin and eosin (H&E) histology of sc tumor sections from each injection group. Original magnification of ×20. Histopathology of sc tumors was performed as described previously (De *et al*., 2003). Injected tibiae were fixed and decalcified overnight in Decalcifier (Surgipath, Richmond, IL, USA), cut longitudinally and embedded in paraffin. Sections (5 *μ*m) were then stained with H&E or subjected to immunohistochemistry with anti-human PSMA (4D8; Northwest Biotherapeutics, Bothell, WA, USA) or a polyclonal rabbit anti-

bovine cytokeratin antibody (Z0622; Dako, Carpinteria, CA, USA) followed by incubation with biotinylated secondaries and developed.

**Table 1**

Changes in bone structural indices of injected tibiae over a 35-day-period

| | BV/TV | | Tb.Th | | Tb.Sp | | Tb.N | | BSA | |
|---|---|---|---|---|---|---|---|---|---|---|
| | **PBS** | **C4-2** | **PBS** | **C4-2** | **PBS** | **C4-2** | **PBS** | **C4-2** | **PBS** | **C4-2** |
| $\alpha v\beta 3$ (—) (4) | -65.23±6.57 | -73.93±7.08 | -26.56±5.38 | -17.06±1.07 | 44.07±6.22 | 105.38±33.21 | -21.87±8.16 | -32.98±11.51 | -49.16±10.27 | -62.71±2.74 |
| $P^1$ | 0.37* | | 0.27 | | 0.25 | | 0.19 | | 0.49 | |
| $\alpha v\beta 3$ WT (4) | -70.62±2.04 | -60.07±9.12 | -20.11±3.82 | -10.77±7.82 | 76.18±25.90 | 52.29±20.56 | -33.03±4.67 | -22.22±4.22 | -56.44±2.35 | -57.27±7.05 |
| $P^1$ | 0.26 | | 0.21 | | 0.27 | | 0.0008** | | 0.92 | |
| $P^2$ | 0.16 | | 0.99 | | 0.049* | | 0.0007** | | 0.40 | |
| $\alpha v\beta 3$ inactive (4) | -52.21±16.03 | -37.42±4.59 | -26.11±1.34 | -8.48±5.39 | 65.52±31.37 | 43.83±18.99 | -21.94±9.95 | -18.56±4.69 | -21.79±28.65 | -10.61±15.37 |
| $P^1$ | 0.35 | | 0.079 | | 0.73 | | 0.72 | | 0.64 | |
| $P^2$ | 0.30 | | 0.48 | | 0.047* | | 0.33 | | 0.40 | |
| $\alpha v\beta 3$ CA (7) | -74.25±5.84 | -62.14±13.04 | -19.50±9.40 | -24.28±8.02 | 75.12±22.09 | 67.35±18.82 | -32.31±4.72 | -28.73±5.74 | -60.86±4.97 | -48.01±14.90 |
| $P^1$ | 0.19 | | 0.45 | | 0.26 | | 0.37 | | 0.35 | |
| $P^2$ | 0.23 | | 0.68 | | 0.16 | | 0.086 | | 0.34 | |

Abbreviations: BSA, bone surface area; PBS, phosphate-buffered saline; BV/TV, % bone in tissue volume; Tb.N, trabecular number; Tb.Sp, trabecular spacing; Tb.Th, trabecular thickness. MicroCT analyses of bone indices were performed within a 1 mm VOI adjacent to the growth plate (number of animals per group are indicated in parenthesis next to groupings). Values for PBS and C4-2 injected tibiae are expressed as %change of index over time of injected tibiae for each animal group. All values are expressed as mean±s.e. Statistical significance was determined using Student's *t*-test as follows. Values were determined by comparing the mean difference (C4-2-PBS control) in increase over time. $P^1$=two-tailed *t*-test for paired samples (C4-2 vs PBS control, same group), $P^2$=two-tailed *t*-test (C4-2 — PBS control) of $\alpha v\beta 3$ (—) group vs the specified group (C4-2 — PBS control)

* $P<0.05$

** $P<0.01$